NSOM Investigation of Carrier Generation, Recombination, and Drift in a Conjugated Polymer

ARTICLE *in* THE JOURNAL OF PHYSICAL CHEMISTRY B · APRIL 2002

Impact Factor: 3.3 · DOI: 10.1021/jp013471w

NSOM Investigation of Carrier Generation, Recombination, and Drift in a Conjugated Polymer

Jason D. McNeill and Paul F. Barbara*

Center for Nano-molecular Science and Technology, Department of Chemistry and Biochemistry, University of Texas, Austin, Texas 78712

Received: September 10, 2001; In Final Form: January 31, 2002

The migration of charge carriers in response to a pulsed electric field was investigated on the 100-nm length scale and microsecond time scale by a recently introduced method employing photoluminescence detection and near field optical excitation through a sharpened optical fiber. A metal coating on the near field probe serves as a ∼100 nm diameter electrode which acts to either collect or repel majority charge carriers, depending on the sign of the applied voltage. The local carrier density is determined by carrier-induced photoluminescence quenching. The transient response is described by a model including carrier drift and diffusion. The role of oxygen in photoinduced carrier generation, exciton quenching, and charge trapping is also investigated.

Introduction

A wide range of electronic and optical device applications employing conjugated polymers and other organic semiconductors as the active material have been developed.[1−3] Conjugated polymer films are known to possess variations in structure and local order on the nanometer length scale which are known to affect their optical end electronic properties.[4−6] Near field scanning optical microscopy (NSOM)[7] is one of few techniques which can extend measurements of electrical and optical properties to the nanometer length scale.[8]

In two previous articles, we introduced a method for indirectly measuring the local charge carrier densities of organic semiconductor films on the ∼100 nanometer length scale.[9,10] The method employs a combination of near field optical excitation through a 50−100 nm diameter aperture, application of a voltage bias to the NSOM probe to create a spatially localized electric field,[11] and detection of local carrier concentration by carrier-induced photoluminescence quenching. The previous data on the conjugated polymer poly[2-methoxy, 5-(2′-ethyl-hexyloxy)-*p*-phenylene-vinylene] (MEH−PPV) indicated that the observed field-induced photoluminescence modulation was a result of photoluminescence quenching by positively charged carriers (hole polarons) within the near field excitation volume. The local concentration of hole polarons was observed to either increase or decrease in response to an electrical bias applied to the NSOM probe.

In this study, we resolve several issues raised by the previous investigation. Organic light-emitting devices typically employ a transparent electrode consisting of indium tin oxide (ITO) as the hole-injecting electrode. To determine the contribution of the ITO electrode to carrier generation and recombination, field-induced photoluminescence modulation results are compared for devices with and without an insulating layer between the MEH−PPV film and the transparent ITO electrode. The results indicate substantial photoinjection of holes at the ITO electrode. Hole recombination at the ITO electrode is also observed. In contrast, when the ITO electrode is covered with an insulating layer, carrier buildup in the MEH−PPV layer occurs. We report the microsecond transient response of carrier density in MEH−PPV upon application of a voltage pulse to the NSOM probe. We present the results of simulations that demonstrate that the transient response serves as a measure of the carrier mobility. The lifetime of photogenerated carriers is probed by measuring the transient response upon modulation of the excitation intensity. The role of oxygen in exciton dissociation and carrier trapping is also explored.

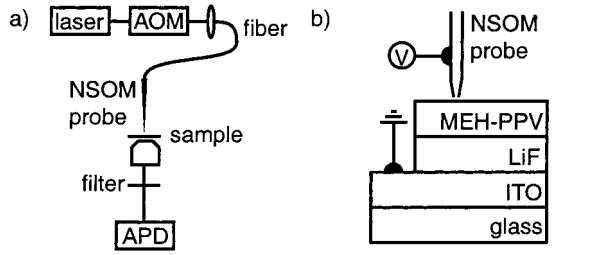

Figure 1. (a) Experimental setup for fluorescence NSOM. AOM: acousto-optic modulator, APD: avalanche photodiode. (b) Sample and probe with connection to function generator for application of electrical pulses.

Experimental Section

Measurements were performed in a modified commercial near field scanning optical microscope (Model Aurora 2 NSOM, ThermoMicroscopes, Inc., Figure 1). Optical excitation of the sample was provided by coupling less than 1 mW of light from an Ar+ laser (488 nm) into a pulled optical fiber. The end of the fiber is coated with ∼100 nm of aluminum resulting in a 50−100 nm diameter aperture. The near field probe is maintained to within a few nanometers of the sample by a piezoelectric scanner under shear force feedback control.[12] The shear force is detected by a 100 kHz piezoelectric tuning fork attached to the probe fiber.[13] The sample photoluminescence is collected by an oil-immersion microscope objective, spectrally filtered with colored glass filters and interference filters to remove light from the excitation laser, and detected using an avalanche photodiode. The microscope is covered with an

* To whom correspondence should be addressed. E-mail: p.barbara@mail.utexas.edu.

10.1021/jp013471w CCC: $22.00
Published on Web 04/11/2002

airtight enclosure for inert gas purging. Experiments were performed in air except where otherwise specified.

Thin films of MEH−PPV (mol. wt. ~10^6, UNIAX Corporation) were spin-cast from an unfiltered solution of MEH−PPV in toluene onto glass coverslips which had been previously coated with indium tin oxide (ITO), a transparent conducting material. The resulting films were approximately 30 nm thick, with a roughness similar to that of the ITO substrate (RMS roughness approximately 4 nm). Images of the topography were qualitatively similar to previously reported results.[10] No clumps or aggregates were observed, in contrast to the results of Nguyen and co-workers[14] that indicated topographic features associated with aggregation. A likely explanation for the discrepancy between our results and the results of Nguyen and co-workers is that the roughness of the ITO substrate employed in the present work would mask any topographic features due to aggregation. Some films were cast onto ITO substrates on which a layer of either LiF or optical grade transparent epoxy had been deposited to electrically insulate the MEH−PPV layer from the ITO electrode. The LiF was deposited by thermal evaporation to a thickness of 5 nm. The epoxy film was fabricated by spin-coating epoxy resin onto the ITO-coated glass substrates, resulting in a thickness of several hundred nanometers. The layer structure of the sample is illustrated in Figure 1b. Comparison of results obtained on samples with and without the insulating layer allows for a comparison of the effects of bulk photoinduced carrier generation and recombination and effects of photoinduced carrier generation and recombination at the ITO interface.

For determination of the transient response to a pulsed electric field, a pulse train consisting of pulses of 1−10 V amplitude, 2−5 ms duration, alternating sign, and a 40% duty cycle was supplied using a programmable function generator. The electrical connection to the Al-coated fiber probe was made using a small amount of conducting epoxy, and the electrical connection to the conducting ITO substrate was made using silver paint. The transient photoluminescence response was recorded using a counter-timer card (National Instruments PCI-6602) synchronized to the function generator and set to a dwell time of 2 microseconds. Application of electrical pulses to the sample resulted in increased electrical noise in the shear force feedback signal. As discussed previously, the effect on the probe-sample distance was a few tenths of a nanometer, and was reduced to less than 0.1 nm by adjusting feedback parameters.[10] No effect due to crosstalk-induced tip motion was observed in the photoluminescence data. The RC time constant due to capacitance of the sample and probe was determined to be less than 100 ns. The photoluminescence count rate was typically in the range of 10−70 kHz. Transients were recorded for 5−20 min and summed to attain an acceptable signal-to-noise ratio. For experiments requiring pulsed laser illumination, the excitation intensity was modulated using an acousto-optic modulator (Model AOM-40, IntraAction Corp.). An extinction ratio of better than one part in 2000 and a switching time of less than 1 microsecond was observed for the acousto-optic modulator.

Results and Discussion

Field-Induced Photoluminescence Modulation. The photoluminescence intensity was determined as a function of applied voltage. The voltage was supplied by a function generator using a voltage ramp waveform. The waveform period was 10 s, sufficiently long to allow the transient response to reach steady state. The waveform was applied repetitively and the photoluminescence was averaged over many cycles in order to obtain an acceptable signal-to-noise ratio. Excitation intensity was varied by a factor of 10 in order to investigate possible effects from carrier recombination or other processes that depend on the excitation rate. To investigate processes occurring at the ITO electrode, identical sets of measurements were performed on MEH−PPV films cast directly on the ITO substrate, and films cast on an epoxy-coated ITO substrate.

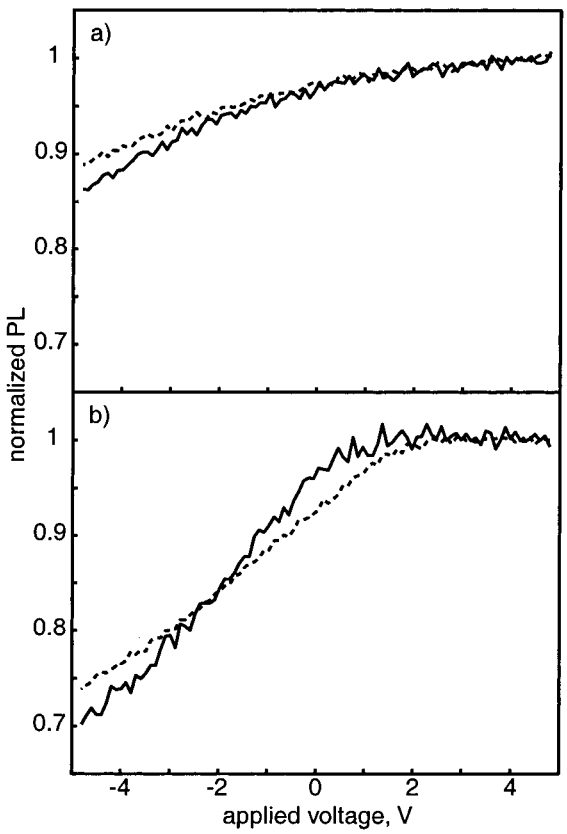

Figure 2. Voltage-dependence of the photoluminescence intensity. Panel (a) is the photoluminescence intensity as a function of tip voltage bias for lower optical excitation intensity (solid line) and higher optical excitation intensity (by a factor of 5, dashed line) for MEH−PPV/ITO. Panel (b) is the photoluminescence intensity as a function of tip voltage bias for lower optical excitation intensity (solid line) and higher optical excitation intensity (by a factor of 5, dashed line) for MEH−PPV/epoxy/ITO. Photoluminescence intensity values are normalized to the intensity at a bias of +5 V.

As previously observed,[10] application of a negative bias to the near field probe causes a reduction in the near field photoluminescence of the MEH−PPV film, whereas the application of a positive bias to the near field probe causes an increase in the near field photoluminescence relative to the photoluminescence obtained at zero bias. For thin films of MEH−PPV spin-cast directly on ITO (Figure 2a), the total modulation over the range between −5 V and +5 V is about 10%. There is little difference between the modulation observed at low and high excitation intensity. We observed an appreciable variability in the magnitude of modulation for samples prepared on different days due to variations in film thickness and morphology. We also find that the magnitude of the voltage-induced photoluminescence modulation depends on the age of the film, which we attribute to slow escape of residual solvent from the film. After 1−2 d of aging, no further change in the field-modulation measurements was detected. All data presented here were collected on samples that had been prepared at least 2 d in advance and stored in a desiccator. The magnitude of modulation was also found to vary from one NSOM probe to

another, but the overall form of the voltage bias-dependence of the photoluminescence was reproducible.

The observed change in photoluminescence is attributed to quenching by hole polarons in the area illuminated by the near field probe.[10,15] Quenching of photoluminescence by hole polarons has been observed in conjugated polymers and other conjugated systems.[15,16] The detailed mechanism by which hole polarons quench singlet excitons in MEH−PPV is not known. It has been observed that hole polarons introduce a red shift in the $\pi - \pi^*$ absorption in conjugated polymers.[17] This should result in efficient Förster energy transfer from singlet excitons to hole polarons. The excited state of the hole polaron has a lower quantum yield of photoluminescence. The net result of the combination of energy transfer and the lower fluorescence quantum yield of the acceptor (the hole polaron) is photoluminescence quenching. Another possible mechanism for quenching of singlet excitons by hole polarons is electron transfer from the singlet exciton to the hole polaron. Both mechanisms are energetically favored. The decrease in photoluminescence upon application of a negative bias to the probe is attributed to collection of hole polarons by the attractive potential well presented by the biased near field probe. The increase in photoluminescence at positive bias is attributed to repulsion of hole polarons resulting in a local depletion of hole polarons.

To investigate processes occurring at the ITO electrode, measurements were also obtained for samples with an insulating epoxy layer between the MEH−PPV film and the ITO electrode, as depicted in Figure 1b. For samples with a thin layer of epoxy, the total modulation is approximately 30% over the range between −5 and +5 V, much larger than the modulation observed for MEH−PPV films in contact with the ITO electrode. The larger modulation indicates a higher polaron concentration when the ITO electrode is covered with an insulating layer. For samples without the insulating layer, hole polaron neutralization at the ITO electrode reduces the hole polaron density. A competing process is increased generation of hole polarons by exciton dissociation at the ITO electrode.[18] For samples fabricated with an insulating layer between the ITO and the MEH−PPV layer, both photoinjection and recombination at ITO are inhibited. In this case, the steady-state concentration of carriers is determined largely by the width and depth of the electrostatic potential well associated with the electrically biased near field probe. This view is consistent with the approximately linear dependence of photoluminescence on voltage over the range of −4 to 0 V.

Imaging Carrier Recombination at a Patterned Electrode. One of the goals of the present work is to develop contrast mechanisms that image device properties on the nanometer length scale. As a demonstration of this capability, field-induced photoluminescence quenching was employed to measure local carrier densities resulting from hole polaron photoinjection and neutralization at ITO in a sample with a patterned electrode. A 5-nm thick layer of LiF was evaporated onto an ITO-coated glass substrate through a TEM grid, which served as a shadow mask. A layer of MEH−PPV was spin-coated on top of the patterned substrate. A pattern of 50 by 50 μm squares indicating regions where LiF had been deposited was clearly visible in the collection objective. An NSOM image was obtained for an area of the sample encompassing the edge of a region coated with LiF. Fluorescence NSOM was recorded while a square wave (5 V amplitude, 125 Hz) was applied to the sample by a function generator. The intensity obtained while a positive bias was applied to the probe (I_+) and the intensity obtained, whereas a negative bias was applied to the probe (I_-) were recorded for each pixel. Images of the average photoluminescence $(I_+ + I_-)/2$ and modulation fraction$2(I_+ - I_-)/(I_+ + I_-)$ are presented in Figure 3. The field-induced modulation is about five times larger in areas where the ITO is covered by the insulating LiF layer than in the area without LiF. The larger modulation over regions with LiF is similar to the larger modulation observed for samples fabricated with an epoxy layer deposited on the ITO electrode. The lower photoluminescence under positive probe bias in the area coated with LiF is attributable to either scattering of the photoluminescence by the LiF layer or a higher concentration of hole polarons over the LiF. The slight offset in the apparent edge position in the image of the modulation possibly indicates the effect of polaron diffusion. When the probe is within a polaron diffusion length of the edge of the LiF layer, polarons diffuse out of the potential well provided by the biased probe. Though no pinholes were identified in the LiF layer, we anticipate that small defects in the LiF film would result in low field-induced PL modulation in an area within a polaron diffusion length of the defect.

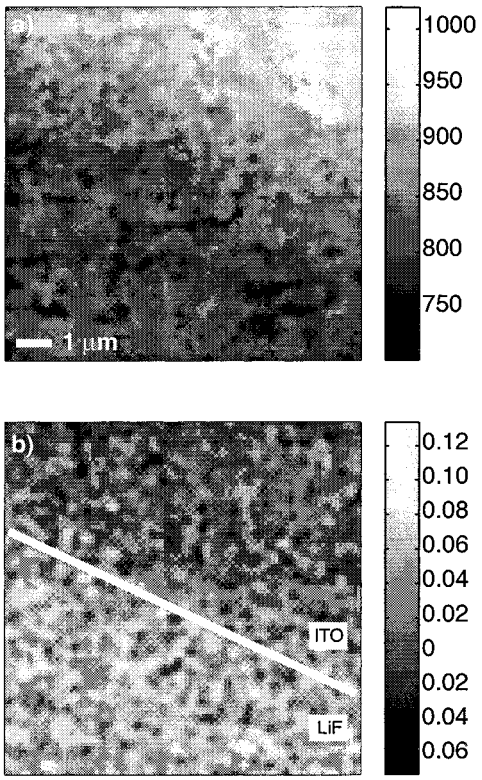

Figure 3. Images of (a) average photoluminescence and (b) field-induced photoluminescence modulation ratio for a patterned sample. The area corresponding to the lower left third of the image has a 5 nm thick layer of LiF between the ITO electrode and the MEH−PPV layer.

Possible effects due to chemical reactions between the LiF layer and the ITO electrode or the MEH−PPV film were investigated. The average photoluminescence obtained in a region coated with LiF while an electrical pulse train of alternating polarity (±5 V) was applied between the probe and the ITO electrode was about the same as the average photoluminescence obtained in the absence of the pulse train. When a train consisting of only −5 V pulses (50% duty cycle, 125 Hz) was applied to the probe, the photoluminescence signal dropped quickly (within a few scan lines) to about 5% of its initial value. Subsequent scans of the same area under zero bias indicated no recovery of the photoluminescence. Reversing the polarity of the pulse train on subsequent scans of the same area also showed no recovery of the photoluminescence, indicating

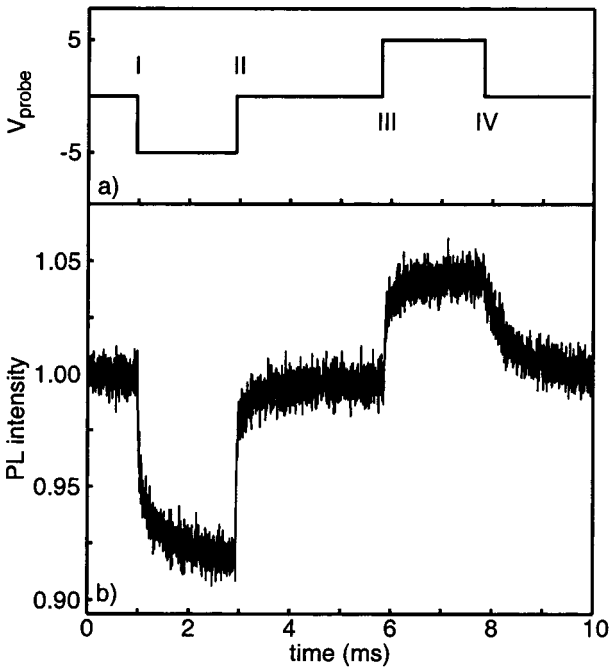

Figure 4. Temporal response of the photoluminescence of MEH−PPV film upon application of a pulse sequence to the probe. Panel (a) depicts the sequence of electrical pulses applied to the near field probe. Panel (b) illustrates the transient response of the photoluminescence.

irreversible damage to the film. The application of a train of −5 V pulses without near field illumination did not result in reduction of the photoluminescence signal obtained during subsequent scans of the same region, indicating sample bleaching involving charged photoinduced species. Regions of the patterned sample without the LiF layer showed no increased damage due to the application of electrical pulses, indicating that LiF is involved in the process which results in damage to the film.

Time-Resolved Photoluminescence Quenching. Figures 4, 5, and 6 illustrate the transient response of the photoluminescence of MEH−PPV to a pulsed electrical bias. The data were collected for a sample consisting of MEH−PPV/epoxy/ITO/glass. A pulse train of alternating polarity was applied to the sample. The waveform applied to the probe and a typical photoluminescence transient are shown in Figure 4. The duration of the pulses was 2 ms, with an off period of 3 ms between pulses. The transient response was averaged over many cycles in order to attain an acceptable signal-to-noise ratio. The transient response upon application and removal of the voltage bias were modeled assuming a biexponential response. The transient response for each portion of the pulse sequence and biexponential fit are shown in Figures 5 and 6. For a given probe, sample, and illumination intensity, the time constants obtained were reproducible. However, the difference between time constants determined for samples prepared on different days was as much as a factor of 5 for the slower component. Upon application of a negative pulse to the probe (0 → −5 V, Figure 5a), there is a noninstantaneous decrease in the photoluminescence. The time constants obtained from a biexponential fit are 26 ± 2 and 520 ± 40 microseconds. Upon removal of the negative voltage from the near field probe (−5 → 0 V, Figure 5b), the photoluminescence increases (recovers) with a biexponential response. The fast component of the turn-off (−5 → 0 V) response (8 ± 1 microseconds) is three times faster than the fast component of the turn-on (0 → −5 V) response. The slow component has a time constant of 340 ± 20 microseconds.

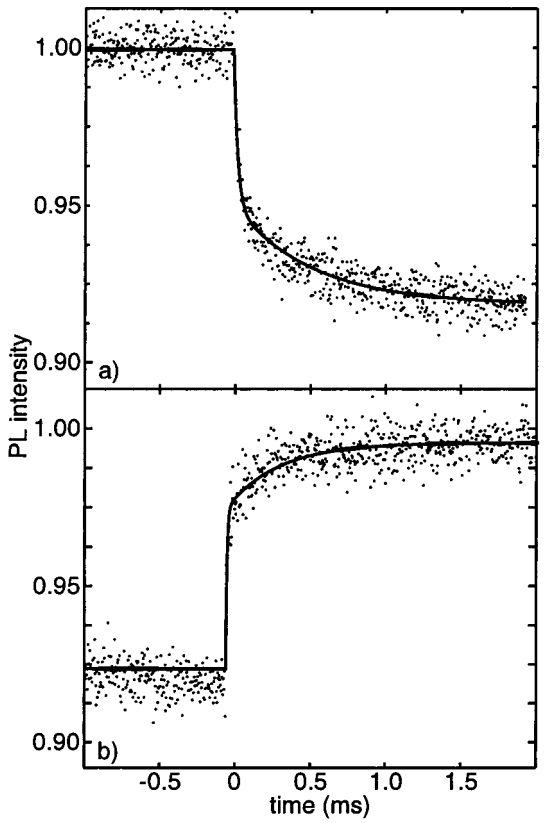

Figure 5. Temporal response of the photoluminescence of MEH−PPV film upon application (a) and removal (b) of a −5 V electrical bias to the near field probe with results of a biexponential fit to the data (solid line). Panels (a) and (b) correspond to labels I and II, respectively, of the pulse sequence in Figure 4. For this sample, the ITO electrode has been insulated from the MEH−PPV layer by a layer of epoxy.

The application of a positive bias to the near field probe results in an increase of the photoluminescence (Figure 6a). The time constants obtained from a fit to a biexponential are 17 ± 2 and 390 ± 50 microseconds. Upon removal of the positive bias (+5 → 0 V, Figure 6b), the photoluminescence slowly drops to the steady-state intensity, with a single-exponential response time of 440 ± 10 microseconds.

It is highly likely that the transient photoluminescence response results from drift of hole polarons toward the voltage-biased probe. This explanation is supported by the fact that the apparent flight time of the hole polarons is similar to simple theoretical estimates. A rough estimate of the flight time may be obtained from the time-of-flight expression $\tau = L^2/\mu V$. If one assumes an average drift distance similar to the probe diameter (approximately 50−100 nm) and a literature value for hole polaron mobility,[19] a flight time in the range of <1 microsecond to a few microseconds is obtained, depending on the field. This is consistent with the fast component of the observed response. A more detailed simulation of hole polaron drift is presented in a later section. In later sections, we investigate other species or processes that may explain the slow component in the transient response.

Pulsed Optical and Electrical Excitation. Although the voltage dependence of the quenching and the transient response indicate the presence of hole polarons, these measurements alone yield no information about the polaron lifetime or generation rate. The measurements described in previous sections were performed repetitively under cw irradiation, which may lead to slow buildup of polarons or other species around the near field

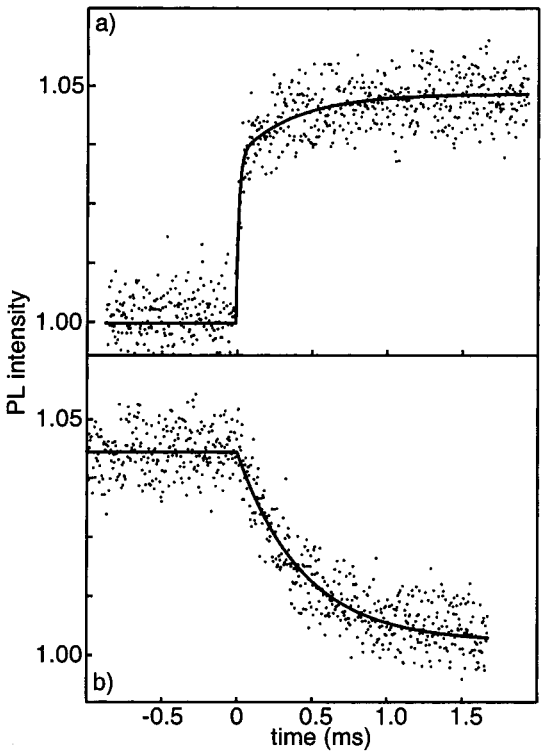

Figure 6. Temporal response of the photoluminescence of MEH−PPV film upon application (a) and removal (b) of a +5 V electrical bias to the near field probe. Panels (a) and (b) correspond to labels III and IV, respectively, of the pulse sequence in Figure 4. For this sample, the ITO electrode has been insulated from the MEH−PPV by a layer of epoxy.

probe. To test whether photogenerated holes persist in the absence of optical excitation, measurements were performed using combined optical and electrical pulses. Measurements were performed on samples of MEH−PPV deposited on epoxy/ITO. The data were acquired using a sequence of two light pulses of 2 ms duration with 3 ms between pulses, as shown in Figure 7a. During the first light pulse of 2 ms duration, 0 V was applied to the probe, whereas the second light pulse was accompanied by a simultaneous electrical pulse applied to the probe. A comparison of the time-resolved photoluminescence data for the first and second pulses is given in panels (b) and (c) of Figure 7. For data acquired when the electrical and optical pulses were simultaneous, the photoluminescence during the second pulse starts at the same level as for 0 V and there is a biexponential response, as observed for pulsed electric fields under continuous illumination. Data were also acquired with the electrical pulse starting 100 microseconds before the start of the second illumination pulse and continuing until the end of the illumination pulse. For the case of the electrical pulse starting prior to the illumination, the initial photoluminescence at the start of the illumination pulse is somewhat lower than the average value for 0 V electrical bias. For data collected with an electrical pulse starting 500 microseconds before the start of the illumination pulse, most of the transient response has apparently occurred before the start of the illumination pulse. For a pulse sequence including a 1 ms duration positive pulse applied to the probe in the interval between illumination pulses, the field-induced response during the second illumination pulse was characterized by a much slower time constant ($\tau = 3.0 \pm 0.5$ ms).

The results clearly indicate polaron drift in the interval between illumination pulses, which is evidence of the persistence

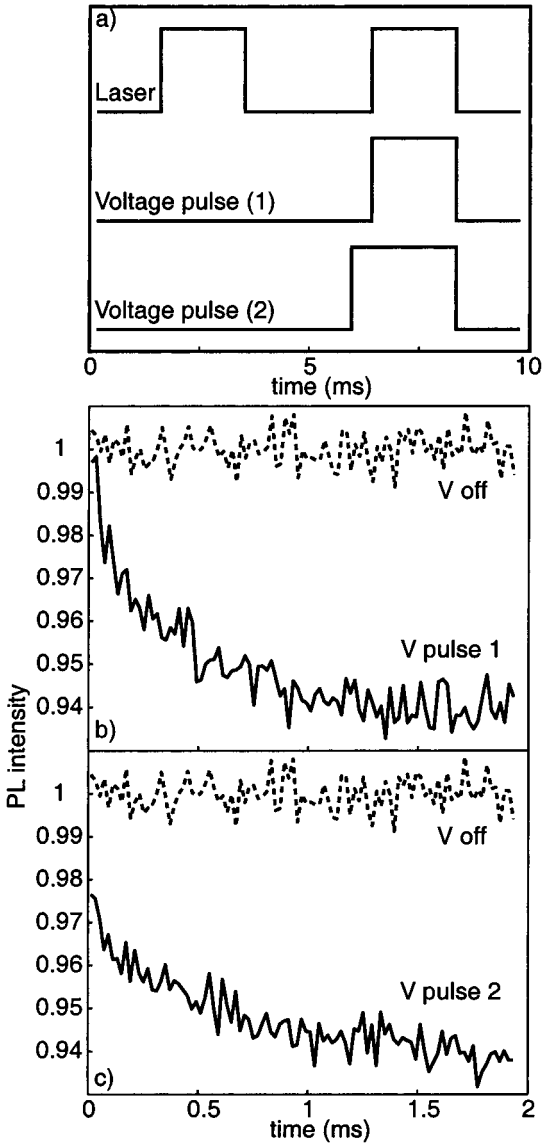

Figure 7. Temporal response of the photoluminescence of MEH−PPV film for a combination of electrical and optical pulses of 2 ms duration. Panel (a) depicts the sequence of illumination and electrical pulses employed in the experiment. In panels (b) and (c), the dashed line is the response without application of electric field (first half of the pulse sequence), whereas the solid line is the response with simultaneous electrical and optical pulses (second half of the pulse sequence). Graph (b) is for a −5 V pulse simultaneous with the illumination pulse. Graph (c) is for a −5 V pulse starting 100 microseconds before the start of the illumination pulse. The difference between (b) and (c) indicates motion of hole polarons prior to illumination.

of carriers during the 3 ms interval between illumination pulses. The holes that drift prior to illumination are persistent hole polarons that were generated during previous illumination pulses. The density of remaining carriers after the interval between the two illumination pulses is apparently reduced, however, by the application of a positive bias to the probe during the interval between light pulses. This result indicates that the persistent hole polarons are swept away from the probe by the positive bias applied in the interval between illumination pulses, considerably slowing drift into the illuminated region during the second illumination pulse.

Transient Response in the Presence of Air Versus Dry Nitrogen. The effect of ambient air on the transient response

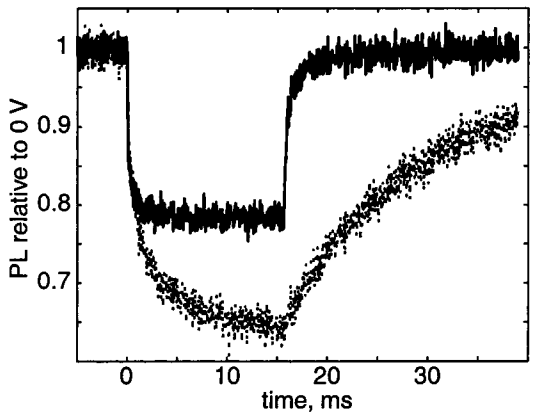

Figure 8. Effect of oxygen on the transient response of the photoluminescence to applied field. The dotted line represents the response to a pulse of −5 V applied to the sample in the presence of ambient air, whereas the solid line represents the response acquired while the apparatus was purged with dry nitrogen.

to alternating electrical pulses was investigated by performing a set of identical field-induced photoluminescence quenching measurements on a sample exposed to air and after purging with dry nitrogen (Figure 8). The airtight enclosure around the microscope was purged for a minimum of 2 h before measurements were performed. The measurements were performed on a thin film of MEH−PPV deposited on epoxy/ITO. In the presence of air, the near field photoluminescence at zero bias is 40% lower compared to the photoluminescence under a nitrogen atmosphere. As shown in Figure 8, the amount of field-induced quenching is increased in the presence of air. Also, there is an increase in the amplitude and time constant of the slower component. This is consistent with a higher density of traps in the presence of oxygen.

The presence of molecular oxygen dissolved in organic semiconductor and polymer semiconductor materials is known to strongly affect their photophysical and electrical properties. For example, exposure to oxygen has been shown to modify the pi-band edge, increase exciton dissociation at ITO electrodes, and alter the work function of metal electrodes.[20,21] Molecular oxygen is also known to behave as an electron acceptor when present in conjugated polymers, forming the superoxide ion (O_2^-) and resulting in p-type doping of the polymer.[21] The lower photoluminescence in the presence of air is attributable to photooxidation, increased carrier generation at defects created by photooxidation,[22,23] collisional quenching,[24] and quenching by MEH−PPV/O_2 charge-transfer complexes.[25] The increase in the slower component is consistent with the presence of traps or carriers with lower mobility. There is also a possibility that mobile O_2^- ions contribute to the observed slow component in the transient response. In either case, it appears that the slow component of the transient response is attributable to the presence of oxygen in the film. Oxygen is also believed to trap electrons, reducing the electron mobility.[26] Extrinsic photoinduced charge generation in the presence of oxygen has also been observed.[21] Though the exact mechanism for enhanced photoinduced charge generation in the presence of oxygen has not yet been established, it is likely that dissociation is an indirect process which involves electron transfer from an exciton to an oxygen molecule, forming O_2^- and a hole polaron. Carbonyl defects on the polymer backbone may also aid exciton dissociation and may additionally serve as traps or recombination centers.

Estimate of Sensitivity of Photoluminescence Quenching to Charge Density. One of the focuses of our research on voltage-biased photoluminescence modulation is the use of this phenomenon as an indirect measure of the local carrier density. In principle, this could be used as a contrast mechanism for imaging charge densities in functioning devices, such as LED's. To obtain a quantitative measure of charge density from these data, however, a calibration of the quenching efficiency vs hole polaron concentration is required. For simplicity we will assume that quenching follows the Stern−Volmer equation[24]

$$\frac{F_0}{F} = 1 + Kn_h, \tag{1}$$

where F_0 is the photoluminescence in the absence of hole polarons, F is the photoluminescence in the presence of hole polarons, n_h is the hole polaron density, and K is the quenching constant. An estimate for K can be obtained from measurements of photoluminescence quenching by holes in thin film devices. Deussen and co-workers measured field-induced photoluminescence quenching in polymer blends of a PPV derivative and polycarbonate.[27] For concentrated blends under forward bias, photoluminescence quenching by hole polarons was observed. Deussen and co-workers used capacitance measurements in order to obtain an estimated polaron density of 5×10^{17} cm^{-3}, and approximately 40% quenching from polarons was observed. This yields a quenching constant, K, of 1.3×10^{-18} cm^3.

We propose that the steady-state PL modulation NSOM for samples fabricated with an insulating layer on top of the ITO electrode also provides a useful system for calibration of the photoluminescence quenching efficiency of a hole polaron. The carrier generation and recombination rates are relatively low because recombination and generation at ITO are blocked. Thus, the potential well presented by the biased probe acts as an electrostatic trap for hole polarons which can be emptied or filled depending on the sign of the bias applied to the probe. We can obtain a rough estimate of the hole density under negative probe bias if we assume that the number of polarons is determined by the width and depth of the potential well presented by the biased probe. We estimate that the number of charges required to fill the potential well under the probe for a 5 V bias on the probe is approximately 500. If we also assume that the charges are confined to a volume of 5×10^{-16} cm^3 (the approximate volume of MEH−PPV directly under the probe), then the resulting approximate hole density is 1×10^{18} cm^{-3}. Because of the complexity of the electric field of the biased probe in close proximity to a semiconducting sample, a solution of the full 3D Poisson−Boltzmann equation is required in order to obtain a more reliable estimate of the hole density. The photoluminescence quenching at −5 V bias is approximately 30%. This yields a quenching constant, K, of 7×10^{-19} cm^3, a factor of 2 smaller than the quenching constant obtained above based on the results of Deussen and co-workers. The closeness of the two values suggests that field-induced photoluminescence modulation NSOM is a useful tool for measuring local hole polaron densities in thin films of conjugated materials and that the quenching constant for a given carrier species is readily obtainable from the data. The density of chromophores, assuming four PPV repeat units per chromophore, is approximately 3×10^{21} cm^{-3}, indicating that a single polaron is capable of quenching photoluminescence in thousands of chromophores. The large quenching volume also indicates that quenching by hole polarons can reduce light-emitting device efficiency at high current densities.

Simulation of Drift-Diffusion and Recombination. Simulations were performed in order to obtain a theoretical estimate of the relative importance of the various factors that may

contribute to the observed transient and steady-state response of the MEH−PPV sample photoluminescence. The transient response of hole polarons for a model system that approximates the experimental configuration was simulated employing a time-dependent drift-diffusion approach, similar to the approach employed in simulations of organic light-emitting diodes.[28] The spatial profile of carriers resulting from generation within the illumination spot, diffusion, and recombination was also investigated. An estimate of the hole polaron density is obtained by comparing transient and steady-state photoluminescence modulation data to the results of model calculations. The effect of carrier recombination at the ITO electrode on the transient response and steady-state carrier density is also modeled.

Drift-diffusion equations for electron and hole transport were employed for a 1D geometry approximating the experimental geometry

$$\mu_e = \mu_{0,e} \exp \sqrt{\frac{E}{E_{0,e}}}, \tag{2}$$

$$\mu_h = \mu_{0,h} \exp \sqrt{\frac{E}{E_{0,h}}}, \tag{3}$$

$$\frac{\partial n_e}{\partial t} = \frac{d}{dx}[\mu_e(E) n_e E] + \frac{d}{dx}\left[D_e(E)\frac{d}{dx}n_e\right] + S - R, \tag{4}$$

$$\frac{\partial n_h}{\partial t} = -\frac{d}{dx}[\mu_h(E) n_h E] + \frac{d}{dx}\left[D_h(E)\frac{d}{dx}n_h\right] + S - R, \tag{5}$$

$$\frac{d^2V}{dx^2} = \frac{q}{\epsilon\epsilon_0}[n_h(x) - n_e(x)], \tag{6}$$

$$R = \frac{q\mu_R}{\epsilon\epsilon_0} n_h n_e, \tag{7}$$

where E is the electric field, $\mu_e$and μ_h are the field-dependent electron and hole mobilities in the Poole-Frenkel form,[29−32] n_e and n_h are the electron and hole densities, $D_e = \mu_e kT/q$ and $D_h = \mu_h kT/q$ are the electron and hole diffusion coefficients, S is the generation rate for carriers, R is the recombination rate for carriers, and μ_R is the recombination mobility, which is the greater of either the electron or hole mobilities.[33] The electrostatic potential in the plane of the sample due to the biased near field probe was assumed to be that of a charged conducting sphere with a radius of 50 nm and a distance from the center of the sphere to the sample plane of 70 nm (Figure 9a). Literature values for the mobility parameters, μ_0 and E_0, were employed.[19] Solutions of the drift-diffusion equations were calculated using a finite difference scheme.[34]

Transient Response of Carriers. The time-dependent response of carriers upon application of a potential bias to the near field probe was calculated. For the results illustrated in Figure 9, a uniform initial carrier distribution was assumed. Carrier generation and recombination were omitted from the calculation. The results of the simulation yield a time-dependent response of n_h in the vicinity of the near field probe that is approximately exponential in form, with a time constant of 23 microseconds, assuming an initial carrier density of 5×10^{17} cm^{-3}. This response time is similar to that of the fast component of the experimental response, indicating that the fast component of the response is consistent with carrier drift under the influence of the electric field presented by the biased near field probe. However, the simulation results do not explain the origin of the slower component of the experimental response. We consider

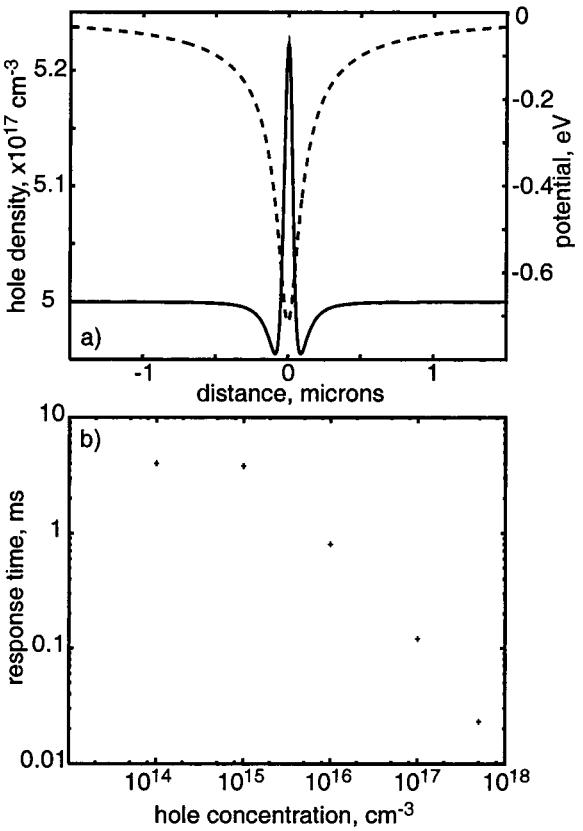

Figure 9. Model electrical potential employed to represent the potential in the plane of the film due to a biased near field probe (Panel a, dashed line). Calculated steady-state hole density for −1 V applied to the probe (Panel a, solid line). Calculated response time for hole polarons as a function of polaron density (b).

two likely mechanisms that may account for the slow component observed in the experimental results: spatial variation in the hole density resulting from diffusion and the presence of low mobility carriers. We neglect micron-scale sample inhomogeneity as a possible cause for the biexponential response because transients obtained in different regions of the sample were similar.

Carrier Diffusion. The simulation results presented in Figure 9 assume a flat initial carrier distribution. However, it is possible that diffusion of photogenerated carriers from the illumination spot would result in a carrier density that decreases with distance from the probe. It is also possible that the carrier density profile resulting from diffusion would give rise to a multiexponential response in the carrier density within the probe volume upon application of a potential bias to the near field probe. We now consider the carrier density profile resulting from the diffusion of photogenerated carriers.

To obtain a qualitative estimate of the carrier concentration as a function of distance from the near field probe, simulations including generation, recombination, and diffusion were performed. Carrier generation is assumed to occur via photoionization in the region of the film illuminated by the sample, and is represented by a Gaussian with a full-width at half-maximum of 50 nm. An important factor in determining the spatial extent of hole polarons is the large disparity in hole and electron mobilities. For simulations in which the hole and electron mobilities are assumed to be equal, the width of the hole density at steady-state is approximately 100 nm. For $\mu_h = 10\mu_e$, which roughly corresponds to measured values for electron and hole mobilities, a fraction of the photogenerated holes diffuses past the slow electrons and avoid recombination. This results in a

very long hole lifetime and the slow accumulation of a broad spatial distribution of holes (fwhm > 600 nm at 0.5 s). The results of the simulation are in qualitative agreement with the long hole polaron lifetime we observed in experiments conducted with modulated illumination (Figure 7). A long diffusion length implies that the concentration of hole polarons at steady state under zero bias within 100 nm of the probe should be relatively constant. Therefore, it is unlikely that spatial variation of the hole polaron density arising from diffusion is responsible for the slow component of the transient response.

Low Mobility Carriers. It is possible that the slow component in the response arises from the presence of a carrier species with a low mobility value. Results obtained from pulsed electrical excitation of organic light-emitting devices indicate a range of mobility values or dispersive transport.[35] The presence of multiple mobility values may be a result of the distribution of energy levels in the sample arising from structural disorder. Transient capacitance measurements have indicated the presence of deep trap levels.[36] The increase in the amplitude of the slow component observed for experiments performed in air as compared to experiments performed in a dry nitrogen atmosphere strongly suggests that the slow component in the transient response is caused by oxygen.

Recombination at ITO. The field-induced photoluminescence modulation for samples fabricated with a layer of epoxy on top of the ITO electrode is several times higher than the modulation measured for samples fabricated with MEH−PPV in direct contact with the ITO. This result is interpreted as an indication that the hole density is lower for MEH−PPV films in contact with ITO. A likely explanation for the lower hole density for films in contact with an electrode surface is that the carrier lifetime is reduced by neutralization at the electrode. An estimate of the effect of recombination at the ITO electrode was obtained by simulating the diffusion of carriers toward a quenching barrier representing the ITO electrode. According to the results of the calculation, the presence of the ITO reduces the steady-state hole density by between 10 and 50%, depending on the charge generation rate. This is consistent with the lower field-induced photoluminescence modulation we observed for MEH−PPV/ITO samples as compared to samples fabricated with an insulating layer between the ITO and the MEH−PPV. Recombination at the ITO electrode should also greatly reduce the in-plane diffusion length for hole polarons.

Conclusions

We have determined the transient response of MEH−PPV photoluminescence to the application of an electrical bias to the near field probe. A modulation of up to 30% was observed which is assigned to exciton quenching by hole polarons. The response time is similar to that obtained from simulations of hole polaron motion under the influence of the electrical potential of the near field probe. This provides additional evidence that the observed photoluminescence modulation upon application of an electrical bias is due to drift and accumulation of hole polarons under the near field probe. The transient response is biexponential, suggesting the presence of at least two distinct species of hole polarons whose mobility values differ by about an order of magnitude. We observe that photogenerated hole polarons persist for several milliseconds. The results of simulations suggest that the persistent hole polarons may result from the much larger mobility of the hole polaron in MEH−PPV, which allows hole polarons to escape recombination with electrons. We also demonstrated imaging of local charge density by field-induced photoluminescence quenching. The imaging results indicated increased carrier buildup in the presence of a buried insulating layer. Exposure to ambient air was shown to both increase the amount of field-induced quenching and increase the amplitude of the slow component of the transient response to a voltage pulse applied to the near field probe. The slow component in the transient response is attributed trapping of hole polarons by oxygen dissolved in the film.

Acknowledgment. We gratefully acknowledge the support of the Robert A. Welch Foundation and the National Science Foundation for support of our NSOM research.

References and Notes

(1) Burroughes, J. H.; Bradley, D. D. C.; Brown, A. R.; Marks, R. N.; Mackay, K.; Friend, R. H.; Burns, P. L.; Holmes, A. B. *Nature* **1990**, *347*, 539.
(2) Braun, D.; Heeger, A. J. *Appl. Phys. Lett.* **1991**, *58*, 1982.
(3) Alivisatos, A. P.; Barbara, P. F.; Castleman, A. W.; Chang, J.; Dixon, D. A.; Klein, M. L.; McLendon, G. L.; Miller, J. S.; Ratner, M. A.; Rossky, P. J.; Stupp, S. I.; Thompson, M. E. *Adv. Mater.* **1998**, *10*, 1297.
(4) Barbara, P. F.; Adams, D. M.; O'Connor, D. B. *Annu. Rev. Mater. Sci.* **1999**, *29*, 433.
(5) Winokur, M. J. Structural Studies of Conducting Polymers. In *Handbook of Conducting Polymers*, 2nd ed.; Skotheim, T., Elsenbaumer, R., Reynolds, J., Eds.; Marcel Dekker: New York, 1998.
(6) Nguyen, T.-Q.; Kwong, R. C.; Thompson, M. E.; Schwartz, B. J. *Appl. Phys. Lett.* **2000**, *76*, 2454.
(7) Betzig, E.; Trautman, J. K.; Harris, T. D.; Weiner, J. S.; Kostelak, L. *Science* **1991**, *251*, 1468.
(8) McNeill, J. D.; O'Connor, D.; Barbara, P. F. *J. Chem. Phys.* **2000**, *112*, 7811.
(9) Adams, D. M.; Kerimo, J.; Liu, C. Y.; Bard, A. J.; Barbara, P. F. *J. Phys. Chem. B* **2000**, *104*, 6728.
(10) McNeill, J. D.; O'Connor, D. B.; Adams, D. M.; Kämmer, S. B.; Barbara, P. F. *J. Phys. Chem. B* **2001**, *105*, 76.
(11) Mei, E.; Higgins, D. A. *J. Phys. Chem. A* **1998**, *102*, 7558.
(12) Toledo-Crow, R.; Yang, P. C.; Chen, Y.; Vaez-Iravani, M. *Appl. Phys. Lett.* **1992**, *60*, 2957.
(13) Karrai, K.; Grober, R. D. *Appl. Phys. Lett.* **1995**, *66*, 1842.
(14) Nguyen, T.-Q.; Martini, I. B.; Liu, J.; Schwartz, B. J. *J. Phys. Chem. B* **2000**, *104*, 237.
(15) Hu, D. H.; Yu, J.; Barbara, P. F. *J. Am. Chem. Soc.* **1999**, *121*, 6936.
(16) Lammi, R. K.; Ambroise, A.; Wagner, R.; Diers, J. R.; Bocian, D. F.; Holten, D.; Lindsey, J. S. *Chem. Phys. Lett.* **2001**, *341*, 35.
(17) Tessler, N. *Adv. Mater.* **1999**, *11*, 363.
(18) Barth, S.; Bässler, H. *Phys. Rev. Lett.* **1997**, *79*, 4445.
(19) Bozano, L.; Carter, S. A.; Scott, J. C.; Malliaras, G. G.; Brock, P. J. *Appl. Phys. Lett.* **1999**, *74*, 1132.
(20) Chawdhury, N.; Kohler, A.; Harrison, M. G.; Hwang, D. H.; Holmes, A. B.; Friend, R. H. *Synth. Met.* **1999**, *102*, 871.
(21) Harrison, M. G.; Gruner, J.; Spencer, G. C. W. *Phys. Rev. B* **1997**, *55*, 7831.
(22) Antoniadis, H.; Rothberg, L. J.; Papadimitrakopolous, F.; Yan, M.; Galvin, M. E.; Abkowitz, M. A. *Phys. Rev. B* **1994**, *50*, 14 911.
(23) Yan, M.; Rothberg, L. J.; Papadimitrakopolous, F.; Galvin, M. E.; Miller, T. M. **1994**, *73*, 744.
(24) Lakowicz, J. R. *Principles of Fluorescence Spectroscopy*; Plenum Press: New York, 1983.
(25) Abdou, M. S. A.; Orfino, F. P.; Son, Y.; Holdcroft, S. *J. Am. Chem. Soc.* **1997**, *119*, 4518.
(26) Papadimitrakopolous, F.; Konstandinidis, K.; Miller, T.; Opila, R.; Chandross, E.; Galvin, M. *Chem. Mater.* **1994**, *6*, 1563.
(27) Deussen, M.; Scheidler, M.; Bassler, H. *Synth. Met.* **1995**, *73*, 123.
(28) Pinner, D. J.; Friend, R. H.; Tessler, N. *J. Appl. Phys.* **1999**, *86*, 5116.
(29) Pai, D. M. *J. Chem. Phys.* **1970**, *52*, 2285.
(30) Gartstein, Y. N.; Conwell, E. M. *Chem. Phys. Lett.* **1995**, *245*, 351.
(31) Dunlap, D. H.; Parris, P. E.; Kenkre, V. M. *Phys. Rev. Lett.* **1996**, *77*, 542.
(32) Meyer, H.; Haarer, D.; Naarman, H.; Horhold, H. H. *Phys. Rev. B* **1995**, *52*, 2587.
(33) Crone, B. K.; Davids, P. S.; Campbell, I. H.; Smith, D. L. *J. Appl. Phys.* **1998**, *84*, 833.
(34) Crank, J. *The Mathematics of Diffusion*, 2nd ed.; Clarendon: Oxford, 1975.
(35) Blom, P. W. M.; Vissenberg, M. C. J. M. *Phys. Rev. Lett.* **1998**, *80*, 3819.
(36) Gomes, H. L.; Stalinga, P.; Rost, H.; Holmes, A. B.; Harrison, M. G.; Friend, R. H. *Appl. Phys. Lett.* **1999**, *74*, 1144.